Available at
www.ComputerScienceWeb.com
POWERED BY SCIENCE DIRECT®

Neurocomputing 52–54 (2003) 97–102

NEUROCOMPUTING

www.elsevier.com/locate/neucom

Synchronization of Purkinje cell pairs along the parallel fiber axis: a model

Sergio Solinas*, Reinoud Maex, Erik De Schutter

Laboratory of Theoretical Neurobiology, Born-Bunge Foundation, University of Antwerp, Wilrijk, Antwerp B-2610, Belgium

Abstract

We build a detailed model of the cerebellar molecular layer taking into account the anatomical, morphological and physiological data available to date. Based on how the percentage of input shared by nearby Purkinje cells (PCs) depends on their relative position in the PC layer we conclude that shared inhibition must play a crucial role in PC synchronization.

Keywords: Cerebellum; Purkinje cells; Synchrony; Interneuron; Inhibition

1. Introduction

Spontaneous synchronization of Purkinje cell (PC) pairs in the cerebellar cortex is implicitly predicted by many theories of cerebellar function (e.g. the beam theory of Eccles [7]). Although the percentage of excitatory and inhibitory input shared by PC pairs can reach 50% and 20%, respectively, short duration positive correlation of in vivo PC simple spike firing has been only rarely observed [6,23]. Here we build a detailed model of the cerebellar molecular layer to investigate the effect of common input on the synchronization of PC pairs.

* Corresponding author.
E-mail address: sergio@bbf.uia.ac.be (S. Solinas).

0925-2312/03/$ - see front matter
doi:10.1016/S0925-2312(02)00846-9

2. Neuron models

2.1. The model Purkinje cell

Our simulations were based on the detailed PC model described previously by De Schutter and Bower [4]. This model represents the morphology of a guinea pig PC [22], and has both passive and active membrane properties. Ten voltage-gated or Ca^{2+}-dependent conductances were modeled: inactivating and persistent Na^+ channels; P-type and T-type Ca^{2+} channels; anomalous inward rectifier, delayed rectifier, persistent, and A-type K^+ channels; Ca^{2+}-activated channels of big-K^+ and K2 types. The model replicates realistic PC firing patterns recorded in vitro during current injection to the soma or dendrites (i.e. simple Na^+ spikes and dendritic Ca^{2+} spikes). Excitatory synaptic input from climbing fibers and parallel fibers (PF) was mediated via AMPA receptor channels. Inhibitory input from molecular layer interneurons (MLI) was mediated via $GABA_A$ receptors channels. In this configuration the model PC fired both dendritic Ca^{2+} spikes, elicited by the synchronous activation of many AMPA receptor channels, and realistic patterns of Na^+ spikes, elicited by a weaker excitatory input. Here, we modified the synaptic parameters to match more recent experimental data [11,21]. The average EPSC recorded in PC somata during stimulation of single granule cells has been fit by a dual exponential function with a peak current of 8.4 pA, a rise time constant of 1 ms and a decay time constant of 1.2 ms [11]. For IPSCs the average values measured 20 pA, 1.6 ms, and 9.3 ms, respectively [21]. These experiments were performed at 32°C [11] and 23°C [21]. We tuned the model PC to 37°C [4] by dividing the AMPA and $GABA_A$ time constants by 1.2 and 1.6, respectively, assuming a Q_{10} factor of 1.5 [1]. Taking into account the temperature dependency of diffusion, the peak conductances were multiplied by the same factors [10]. The synaptic peak conductances needed to generate the experimental somatic current amplitudes were recalculated in the model PC during simulated voltage clamp of the soma (holding potential −70 mV [2] and −60 mV [21], respectively), correcting this way for the incomplete space clamp of the dendritic tree and for the low input resistance of the model PC [5]. To achieve the average somatic currents measured in vitro we had to multiply the AMPA and $GABA_A$ peak conductances by a factor of 9 and 6, respectively. The final parameters were: AMPA channels peak conductance 1.3 nS, rise and decay time constants 0.6 and 1 ms, peak somatic EPSC 10 pA; $GABA_A$ channels peak conductance 3 nS, rise and decay time constants 1 and 5 ms, peak somatic IPSC 32 pA. After these corrections the model PC still replicates in vivo firing patterns. Synaptic plasticity or probability of release were not modeled.

2.2. The model molecular layer interneuron

The molecular layer interneuron (MLI: stellate or basket cell) was modeled as an isopotential spherical soma with a diameter of 10 μm [14]. A specific membrane resistance of 12.5 kΩ cm^2 [14] and a specific membrane capacitance of 1 μF/cm^2 [14] gave a passive membrane time constant of 13.5 ms [9]. The model had six types of active membrane channels: inactivating Na^+ channels, high-voltage-activated Ca^{2+} channels,

delayed rectifier and A-type K^+ channels, KC Ca^{2+}-activated K^+ channels, and anomalous inward rectifier Na^+/K^+ channels. These channels were borrowed from a Golgi cell model described previously [15], since MLIs and Golgi cells have indistinguishable electrophysiological properties in vitro [18]. We tuned the model MLI to achieve a spontaneous firing rate of 18 spikes/s [9] by increasing the reversal potential of the leak current to −46 mV. The synaptic input was provided by AMPA [3] and $GABA_A$ [12] receptor channels. The peak EPSC is a free parameter of our model, the only constraint being that a single EPSC should be able to elicit a post-synaptic spike (M. Häusser, personal communication). The EPSC time course can be fit by an α-function with a time constant of 1.5 ms at 23°C [3]. The peak IPSC measures in vitro 60 pA at 21°C [12] (holding potential −60 mV, pipette filled with high Cl^- concentration solution) and the channel opening and closing time constants are 0.3 and 10.5 ms [12], respectively. We tuned the model to 37°C by dividing the AMPA and $GABA_A$ time constant by 1.8 and 1.9, respectively, and multiplying the $GABA_A$ channel peak conductance by 1.9 [10]. The final parameters were: AMPA channels peak conductance 200–400 pS, time constant 0.8 ms; $GABA_A$ channels peak conductance 1.9 nS, rise and decay time constants 0.16 and 5.5 ms, peak somatic IPSC 110 pA. Synaptic plasticity or probability of release were not modeled.

3. A local network for each Purkinje cell

In the cerebellar cortex the MLIs surround the PC dendritic tree (density 32,000 cells/mm^3 [8,13]) making GABAergic synapses onto them. The stellate cells contact the PC spiny thick dendrite. The basket cell axons make synapses onto the PC main dendrite or surround their somata with a characteristic basket like structure [19]. Both MLI dendrites and axons are mainly confined to the cerebellar sagittal plain, making only short extensions along the PF axis. The volume spanned by the dendrite (PF axis 16 μm, sagittal axis 174 μm, radial axis 140 μm) is centered on the soma while the center of the axonal volume (PF axis 50 μm, sagittal axis 266 μm, radial axis 100 μm) is dislocated by 150 μm along the sagittal axis [24]. We calculated the upper limit for the volume of the presynaptic inhibitory basin of a PC, i.e. the volume containing all the MLIs whose axons reach the PC dendritic tree. The extension of the basin along the sagittal axis equals the depth of the PC dendritic tree, 250 μm [19], plus twice the length of an MLI axon, 250 μm. Along the PF axis, the extension measures the width of the PC dendritic tree (5 μm) plus twice 50 μm. The height of our approximative PC presynaptic basin is the average thickness of the molecular layer (300 μm). From this, the basin measured 750 μm by 105 μm by 300 μm and contains approximately 750 MLIs. Conversely, an MLI axon contacts on average 15 PCs [24], and given that in the cerebellar cortex there are appropriately 10 MLIs per PC [13], each PC should receive input from 150 MLIs. Thus, each MLI inside the basin connected to the PC with a probability of 0.2. In our network model each MLI within the PC presynaptic basin had the same probability of making a synapse and the number of MLIs presynaptic to a PC is fixed to 150. Out of these, 50 MLIs from the inner third of the molecular layer connected like basket cells to single $GABA_A$ synapses on the

PC main dendrites or soma. The other 100 MLIs made on average nine synapses on the PC spiny and thick dendritic compartments like stellate cells do [24]. For these synapses, the synaptic strength was divided by the average number of contacts. From slice recordings it is known that MLIs are interconnected with each other through an average of four inhibitory synapses [12]. Since in slices some MLI axons and dendritic trees might be injured, we took this figure as a lower bound. Therefore, in our model the MLIs were coupled by an average of 10 synapses, with synaptic strength normalized by 10.

3.1. The excitatory input

In the cerebellar cortex, both PCs and MLIs receive excitatory input from granule cell axons, which originate in the granular layer and rise to the molecular layer. There they bifurcate and run parallel to each other and orthogonal to the sagittal plane giving origin to the parallel fiber system. The cerebellar granule cell population is the largest of the central nervous system. Because it is currently impossible to simulate billions of cells, we assume that only 1% of the granule cells is active at rest, which is in agreement with recent in vivo recordings [16]. Since a real PC has 175,000 PF synapses [8] the 1474 spines in our model sufficed to receive this reduced granule cell input. The same holds for MLIs, we calculated that in real animals they receive 1500 PF synapses [8] and in our simulations only 15. At the present stage of implementation the excitatory input to the PCs and MLIs is provided by random spike train generators. These elements were placed at the PF bifurcation points and connected only to AMPA channels within 2.5 mm along the PF axis and 20 μm in the other two directions [20]. The PF conduction speed was set to 0.5 m/s [17].

3.2. What inputs do Purkinje cells share?

Synchronization of in vivo PC simple spikes has only rarely been reported. In particular for wild type animals short duration correlation, within 100 ms, has not been reported for PCs separated by more than 100 μm [6,23]. Based on anatomical data [8,24] we calculated the percentage input shared by two PCs as a function of their relative position in the PC layer. Fig. 1 shows the linear drop in shared input for increasing distance between the PC somata. Adjacent PCs should share about 50% of their afferent PFs and 20% of their presynaptic MLIs, since the respective connection probabilities are 0.5 [8] and 0.2 (see above). For a PC pair aligned along the PF axis the percentage of shared excitation vanishes at the length of the PFs (i.e. 5 mm) and the percentage of shared inhibition at the depth of the inhibitory basin (i.e. 100 μm). With respect to the sagittal axis common inhibitory input is available over a broader range than shared excitation. Two PCs separated by a distance between 250 and 375 μm along the sagittal axis would still share part of their inhibition but none of their excitatory input.

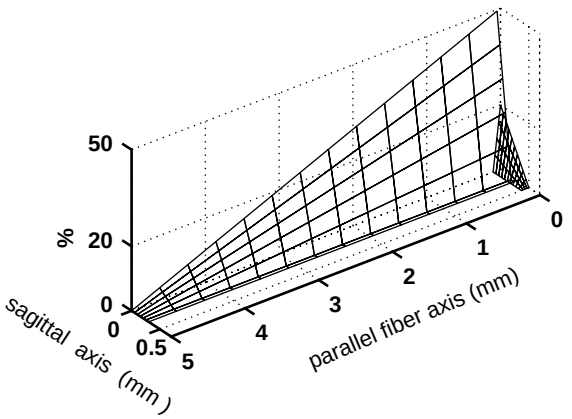

Fig. 1. Two PCs share a variable percentage of their input depending on their relative location. The plot shows the percentage of excitatory (full lines) and inhibitory (dot–dashed lines) input shared by two PCs, one positioned in the origin and another with somatic coordinates reported on the two horizontal axes.

4. Conclusions

We conclude that the common PF input to pairs of PC might not be strong enough to induce significant synchronous firing through a monosynaptic pathway. On the other hand, the common inhibitory input to PCs separated by at most 100 μm should induce synchronous firing. Nevertheless, synchronization of PCs separated by a longer distance along the PF axis may still be achieved through a disynaptic pathway.

Acknowledgements

Supported by EC QLRT-2000-02256 and HFSP RG0091/1999-B.

References

[1] P.P. Atluri, W.G. Regehr, Determinants of the time course of facilitation at the granule cell to Purkinje cell synapse, J. Neurosci. 16 (1996) 5661–5671.
[2] B. Barbour, Synaptic currents evoked in Purkinje cells by stimulating individual granule cells, Neuron 11 (1993) 759–769.
[3] B. Barbour, B.U. Keller, I. Llano, A. Marty, Prolonged presence of glutamate during excitatory synaptic transmission to cerebellar Purkinje cells, Neuron 12 (1994) 1331–1343.
[4] E. De Schutter, J. Bower, An active membrane model of the cerebellar Purkinje cell. I. Simulation of current clamps in slice, J. Neurophysiol. 71 (1994) 375–400.
[5] E. De Schutter, J. Bower, An active membrane model of the cerebellar Purkinje cell. II. Simulation of synaptic responses, J. Neurophysiol. 71 (1994) 401–419.
[6] T.J. Ebner, J.R. Bloedel, Correlation between activity of Purkinje cells and its modification by natural peripheral stimuli, J. Neurophysiol. 45 (1981) 948–961.
[7] J.C. Eccles, M. Ito, J. Szentágothai, The Cerebellum as a Neuronal Machine, Springer, Berlin, 1967.

[8] R.J. Harvey, R.M. Napper, Quantitative studies on the mammalian cerebellum, Prog. Neurobiol. 36 (1991) 437–463.
[9] M. Häusser, B.A. Clark, Tonic synaptic inhibition modulates neuronal output pattern and spatiotemporal synaptic integration, Neuron 19 (1997) 665–678.
[10] B. Hille, Ionic Channels of Excitable Membranes, Sinauer, Sunderland, Massachusetts, 1991.
[11] P. Isope, B. Barbour, Properties of unitary granule cell-Purkinje cell synapses in adult rat cerebellar slices, J. Neurosci. 15 (2002) 9668–9678.
[12] S. Kondo, A. Marty, Synaptic currents at individual connections among stellate cells in rat cerebellar slices, J. Physiol. 509 (1998) 221–232.
[13] L. Korbo, B.B. Andersen, O. Ladefoged, A. Møller, Total numbers of cell types in rat cerebellar cortex estimated using an unbiased stereological method, Brain Res. 609 (1993) 262–268.
[14] I. Llano, H.M. Gerschenfeld, Inhibitory synaptic currents in the stellate cells of rat cerebellar slices, J. Physiol. 468 (1993) 177–200.
[15] R. Maex, E. De Schutter, Synchronization of golgi and granule cell firing in a detailed network model of the cerebellar granule cell layer, J. Neurophysiol. 80 (1998) 2521–2537.
[16] T. Margrie, M. Häusser, Patch clamp recordings from cerebellar granule cells in vivo, 3rd Forum of European Neuroscience—Abstract Book, 2002, p. 126.12.
[17] E.G . Merril, P.D. Wall, T.L. Yaksh, Properties of two unmyelinated fibre tracts of the central nervous system: lateral Lissauer tract, and parallel fibres of the cerebellum, J. Physiol. 284 (1978) 127–145.
[18] J. Midtgaard, Membrane properties and synaptic responses of Golgi cells and stellate cells in the turtle cerebellum, J. Physiol. 457 (1992) 329–354.
[19] S.L. Palay, V. Chan-Palay, Cerebellar Cortex, Springer, Berlin, 1974.
[20] C. Pichitpornchai, J.A. Rawson, S. Rees, Morphology of parallel fibres in the cerebellar cortex of the rat: an experimental light and electron microscopic study with biocytin, J. Comp. Neurol. 342 (1994) 206–220.
[21] C. Pouzat, S. Hestrin, Developmental regulation of basket/stellate cell → Purkinje cell synapses in the cerebellum, J. Neurosci. 17 (1997) 9104–9112.
[22] M. Rapp, I. Segev, Y. Yarom, Physiology, morphology and detailed passive models of guinea-pig cerebellar Purkinje cells, J. Physiol. 474 (1994) 101–118.
[23] S.-L. Shin, V. Steuber, P. Fagerstedt, E. De Schutter, Correlation of simple spike activity in cerebellar Purkinje cells, Soc. Neurosci. Abstr. 2001, p. 294.2.
[24] F. Sultan, J.M. Bower, Quantitative Golgi study of the rat cerebellar molecular layer interneurones using principal component analysis, J. Comp. Neurol. 393 (1998) 353–373.